Polymer Degradation and Stability 113 (2015) 22–31

Contents lists available at ScienceDirect

Polymer Degradation and Stability

journal homepage: www.elsevier.com/locate/polydegstab

Flame-retardant mechanism of a novel polymeric intumescent flame retardant containing caged bicyclic phosphate for polypropylene

Xuejun Lai*, Shuang Tang, Hongqiang Li, Xingrong Zeng*

College of Materials Science and Engineering, South China University of Technology, Guangzhou 510640, People's Republic of China

ARTICLE INFO

Article history:
Received 26 September 2014
Received in revised form
22 December 2014
Accepted 12 January 2015
Available online 22 January 2015

Keywords:
Polymeric intumescent flame retardant
Polypropylene
Caged bicyclic phosphate
Single-component
Flame-retardant mechanism

ABSTRACT

A novel polymeric intumescent flame retardant, named poly(ethanediamine–1,3,5-triazine-*o*-bicyclic pentaerythritol phosphate) (PETBP), was synthesized and characterized by Fourier transform infrared spectroscopy (FTIR), solid-state ^{13}C nuclear magnetic resonance (^{13}C NMR), ^{31}P NMR and elemental analysis (EA). The effects of PETBP on the flame retardancy and thermostability of polypropylene (PP) were investigated by limiting oxygen index (LOI), vertical burning test (UL-94V), cone calorimetric test (CCT), thermogravimetric analysis (TGA) and TG-FTIR, respectively. The results showed that PETBP could significantly improve the flame retardancy and thermostability of PP. When the content of PETBP was 25.0 wt%, the PP/PETBP mixture could achieve a LOI value of 29.5% and a UL-94 V-0 rating, and its peak heat release rate (PHRR), total heat release (THR), average mass loss rate (av-MLR), smoke production rate (SPR) and total smoke production (TSP) were considerably decreased. The flame-retardant mechanism of PETBP was investigated by TGA, FTIR, TG-FTIR and scanning electron microscopy-energy dispersive X-ray spectrometry (SEM-EDXS). The results revealed that during the combustion PETBP could quench the free radicals of PP chain scission, and form a continuous and compact intumescent char on the substrate, thus effectively retard the degradation and combustion of PP.

© 2015 Elsevier Ltd. All rights reserved.

1. Introduction

Polypropylene (PP) is a widely used thermoplastic in many fields due to its easy processing capability, excellent mechanical performance and low cost. However, the inherent flammability is a major drawback of PP and severely restricts its application in some aspects required high flame retardancy. Therefore, it is imperative to improve the flame retardancy of PP. In recent years, intumescent flame retardant (IFR) is considered to be one of the most promising flame retardants to replace halogen-containing ones, because of them being environmental-friendly, having high efficiency, anti-dripping and low smoke [1–3]. Typically, IFR consists of three ingredients, including an acid source, a charring agent and a blowing agent. The most commonly reported IFR is ammonium polyphosphate/pentaerythritol/melamine (APP/PER/MEL), which has been systematically investigated by Camino's and Bourbigot's groups [1,4–6]. Their researches revealed that the IFR could form a multicellular swollen char on the surface of the polymer when being heated beyond a critical temperature, which protected the substrate from burning. However, the traditional IFRs are mainly composed of small molecule compounds, such as PER and MEL, which are moisture sensitive and easily attacked by water and exuded out of the mixtures, leading to a severe deterioration of the flame retardancy [7,8].

One solution to these problems is to employ microencapsulation technology by enveloping the IFR particles in a thin film of polymer which serves as a solid wall [7–11]. The other one is to synthesize polymeric IFRs with high molecule weight, which possess low water solubility and better resistance to extraction [12–14]. Song and Co-workers [14] synthesized an oligomeric intumescent flame retardant, named PDBPP, and employed it to flame retard PP. The results showed that the incorporation of PDBPP could improve both the flame retardancy and thermostability of PP. However, in order to achieve a limiting oxygen index (LOI) value of 28.0%, more than 30wt% PDBPP was necessary. The relatively low flame retardant efficiency limited its further application. In recent years, triazine derivatives have aroused more and more attention because of their high reactivity and good char-forming performance [15–17]. Our

* Corresponding authors. College of Materials Science and Engineering, South China University of Technology, No 381, Wushan Road, Tianhe District, Guangzhou 510640, China. Tel./fax: +86 20 87114248.
E-mail addresses: msxjlai@scut.edu.cn (X. Lai), psxrzeng@gmail.com (X. Zeng).

http://dx.doi.org/10.1016/j.polymdegradstab.2015.01.009
0141-3910/© 2015 Elsevier Ltd. All rights reserved.

group [18] had reported a novel charring agent triazine-based macromolecule (TBM), which showed a superior char-forming capability and little water solubility. Nevertheless, owing to the absence of acid source, TBM was still needed to combine with melamine pyrophosphate (MPP) to obtain good flame retardancy, which required more complicated processing condition to achieve uniform dispersion of the IFR particles in the polymer.

In this work, a novel single-component polymeric IFR containing caged bicyclic phosphate, named poly(ethanediamine-1,3,5—triazine-*o*-bicyclic pentaerythritol phosphate) (PETBP), was synthesized by using phosphorus oxychloride, pentaerythritol, cyanuric chloride and ethylenediamine. The chemical structure of PETBP was characterized by Fourier transform infrared spectroscopy (FTIR), solid-state ^{13}C nuclear magnetic resonance (^{13}C NMR), ^{31}P NMR and elemental analysis (EA). The flame retardancy, thermal properties and flame-retardant mechanism of the PP/PETBP mixture were investigated by limiting oxygen index (LOI), vertical burning test (UL-94V), cone calorimetric test (CCT), thermogravimetric analysis (TGA), thermogravimetry-Fourier transform infrared spectrometry (TG-FTIR), and scanning electron microscopy-energy dispersive spectra (SEM-EDXS).

2. Materials and experimental

2.1. Materials

Phosphorus oxychloride ($POCl_3$) was provided by Guangzhou Chemical Reagent Co., Ltd., China. $POCl_3$ was distilled under atmospheric pressure before use. Pentaerythritol (PER, water solubility at 70 °C: 15.0 g/100 mL H_2O) was purchased from Tianjin Kermel Chemical Reagent Co. Ltd., China. Ammonium polyphosphate (APP, water solubility at 70 °C: 2.5 g/100 mL H_2O) and melamine pyrophosphate (MPP, water solubility at 70 °C: 1.3 g/100 mL H_2O) was obtained from Jiangmen Topchem Technology Co., Ltd., China. Triazine-based macromolecule (TBM, water solubility at 70 °C: 0.7 g/100 mL H_2O) was synthesized according to the reference [18]. Cyanuric chloride (CNC) was obtained from Yingkou Sanzheng Organic Chemical Industry Co., Ltd., China. Ethanediamine was obtained from Chinasun Specialty Products Co., Ltd., China. Acetonitrile and triethylamine were obtained from China National Pharmaceutical Group, China. Polypropylene (PP, T30S), a granulated product with a melt flow index of 3.0 g/10 min (230 °C, 2.16 kg), was supplied by Maoming Petrochemical Co., Ltd., China. Antioxidant (IRGANOX B215) was provided by Ciba Specialty Chemicals Inc., Switzerland. 2,6,7-Trioxa-1-phosphabicyclo-[2,2,2] octane-4-methanol-1-oxide (PEPA, as shown in Scheme 1) was synthesized according to the reference [19] and recrystallized in alcohol. All the commercial materials except $POCl_3$ were used directly without further purification.

2.2. Synthesis of poly(ethanediamine-1,3,5—triazine-o-bicyclic pentaerythritol phosphate) (PETBP)

Exactly 36.9 g (0.2 mol) cyanuric chloride and 150 mL acetonitrile were added in a 500 mL round bottom flask under nitrogen, and stirred at room temperature until a transparent solution was formed. Then, 36.0 g (0.2 mol) PEPA and 27.8 mL (0.2 mol) triethylamine were dissolved in another 100 mL acetonitrile. The mixture solution was dropped slowly into the flask. The pH value of the solution was monitored in real time by a pH measuring apparatus (SX723, Shanghai San-Xin Instrumentation, Inc.) and kept at 7—8. The reaction was continued for 4 h after the mixture solution was dropped completely. Afterwards, the temperature was increased to 45—50 °C. 6 g (0.1 mol) ethanediamine and 27.8 mL

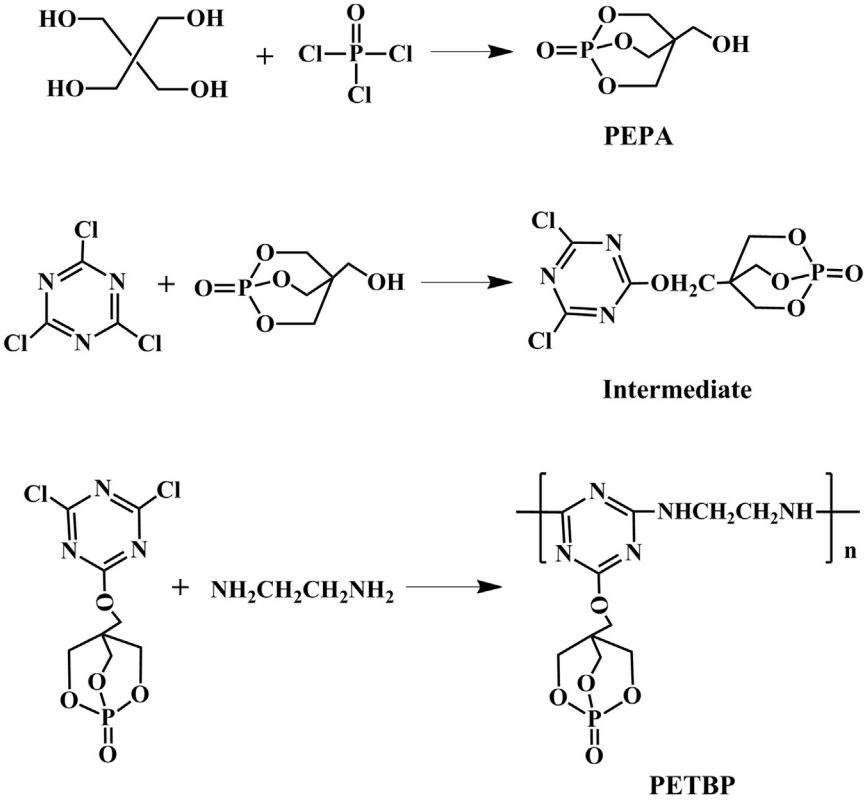

Scheme 1. Synthetic route of PETBP.

(0.2 mol) triethylamine were added dropwise into the flask (the pH was kept at 7–8). The reaction was lasted for another 4 h. Then, the temperature was heated up to reflux temperature. Another solution containing 6 g (0.1 mol) ethanediamine and 27.8 mL (0.2 mol) triethylamine were added dropwise into the flask (the pH value was also kept at 7–8), and the reaction was kept under reflux for 6 h. The precipitate was then washed with distilled water and acetone for each three times. After dried at 100 °C under vacuum to a constant weight (yield: 81.7%), the white powdery PETBP was obtained. The chlorine content of PETBP was less than 40 ppm. The degree of polymerization for PETBP was about 47 (number-average molecular weight was 14800). The water solubility of PETBP at 25 °C and 70 °C was 0.5 g/100 mL H_2O and 0.9 g/100 mL H_2O, respectively. The synthetic route of PETBP was shown in Scheme 1.

2.3. Preparation of flame retardant PP

PP, APP, PER, MPP, TBM and PETBP were dried in a vacuum oven at 80 °C for 3 h before use. Then PP and flame retardants were melt-blended on a two-roll mill (XK-160, Changzhou Shuangfeng Machinery Factory, China) at 170 °C for 15 min. The prepared mixtures were molded under compression (15 MPa) at 180 °C for 6 min and cooled to room temperature naturally to obtain flame retardant PP sheets with standard size for further testing.

2.4. Characterization and measurement

2.4.1. Fourier transform infrared spectrometry (FTIR)

The sample was mixed with KBr powder, and then pressed into a tablet. The FTIR spectrum of the sample was recorded on a Tensor 27 spectrometer (Bruker Optics Inc., Germany) by averaging 16 scans at a resolution of 4 cm^{-1}. The measurement was carried out in the optical range of 4000–400 cm^{-1}.

2.4.2. Nuclear magnetic resonance spectrometry (NMR)

The solid-state ^{13}C NMR and ^{31}P NMR (using 85% H_3PO_4 as reference and d_6-DMSO as solvent) spectra of the sample were recorded on an AVANCE AV-400 Fourier transform superconducting magnetic resonance spectrometer (Bruker Inc., Germany).

2.4.3. Gel permeation chromatography (GPC)

GPC was carried out on a Waters 2410 gel permeation chromatography (Waters Inc., USA) at 30 °C dimethylsulfoxide (DMSO) as the solvent and narrowly distributed polystyrene (PS) as the standard.

2.4.4. Elemental analysis (EA) and inductively coupled plasma-atomic emission spectrometry (ICP-AES)

The element content of the sample was measured by an elemental analyzer (Vario EL cube, Elementar Analysensysteme GmbH, Germany) and an inductively coupled plasma-atomic emission spectrometer (ICAP 6500 Duo, ThermoFisher Scientific Co., USA).

2.4.5. X-Ray fluorescence spectrometer (XRFS)

The chlorine content of the sample was measured by an X-Ray fluorescence spectrometer (Axios Pw4400, Panalytical B.V. Co., Netherlands).

2.4.6. Thermogravimetric analysis (TGA)

The TGA was carried out with a TG209 thermal analyzer (Netzsch Instruments Co., Germany) from 30 °C to 700 °C at a linear heating rate of 20 °C/min under an air flow of 30 mL/min. Each sample was measured in an alumina crucible with a weight about 10 mg.

2.4.7. Thermogravimetry-Fourier transform infrared spectrometry (TG-FTIR)

The TG-FTIR instrument consists of a thermogravimeter (TG209, Netzsch Instruments Co., Germany), a Fourier transform infrared spectrometer (Tensor 27, Bruker Optics Inc., Germany), and a transfer tube with an inner diameter of 1 mm connected the TG and the infrared cell. The investigation was carried out from 30 °C to 750 °C at a linear heating rate of 20 °C/min under a nitrogen flow of 30 mL/min. In order to reduce the possibility of pyrolysis gas condensing along the transfer tube, the temperature of the infrared cell and transfer tube was set to 230 °C.

2.4.8. Limiting oxygen index (LOI)

The LOI values were measured by an oxygen index meter (HC-2, Jiangning Analysis Instrument Co., China) according to ASTM D

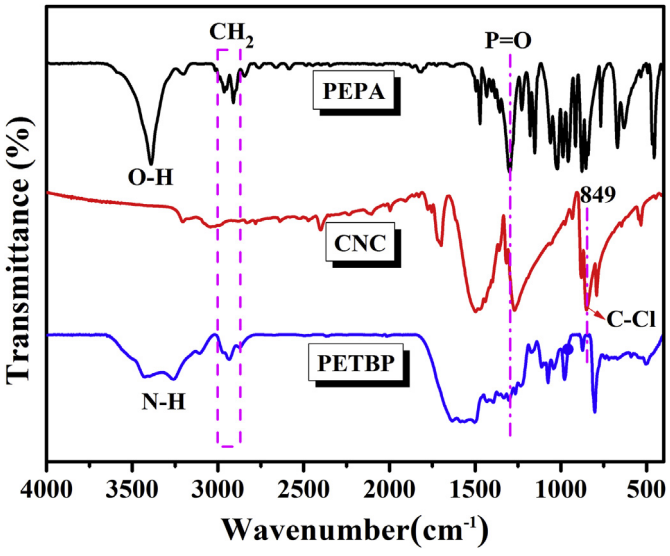

Fig. 1. FTIR spectra of PEPA, CNC and PETBP.

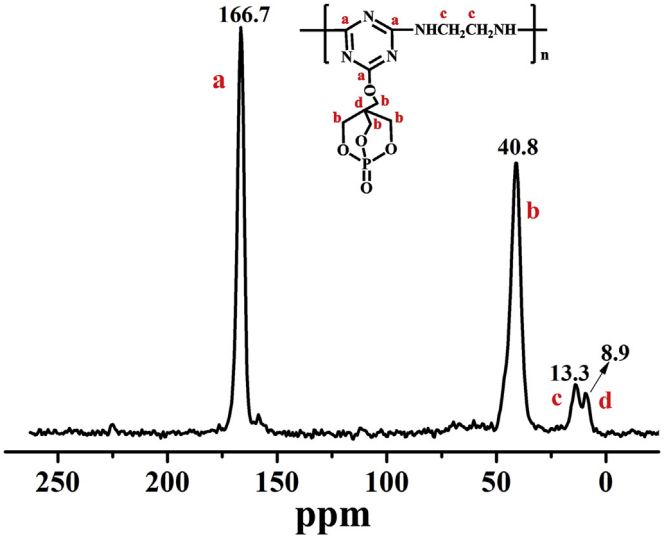

Fig. 2. Solid-state ^{13}C NMR spectrum of PETBP.

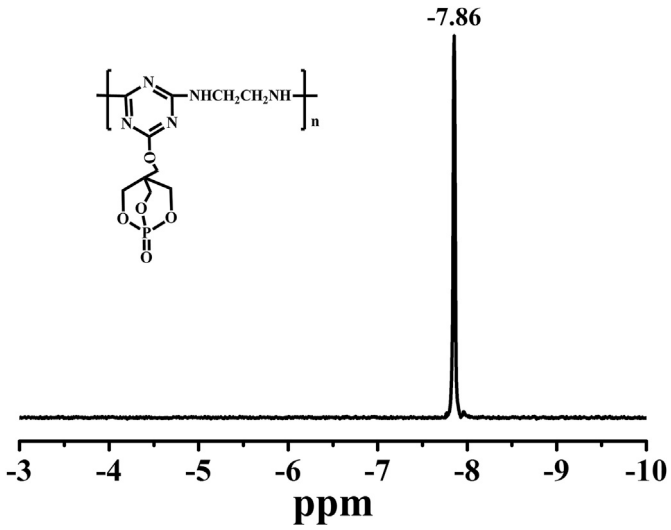

Fig. 3. ^{31}P NMR spectrum of PETBP.

2863–2008. The dimensions of the specimens were 80 mm × 10 mm × 4.0 mm.

2.4.9. Vertical burning test

The vertical burning test was conducted on a vertical burn instrument (CFZ-3, Jiangning Analysis Instrument Co., China) according to the UL-94 vertical test standard (ASTM 3801-2010). The dimensions of the specimens were 127 mm × 12.7 mm × 3.2 mm.

2.4.10. Cone calorimetric test (CCT)

The CCT was carried out by using a cone calorimeter (Fire Testing Technology Co., UK) according to ISO5660. Each specimen, with the dimensions of 100 mm × 100 mm × 4.0 mm, was wrapped in aluminum foil and exposed horizontally to an external heat flux of 35 kW/m^2. All samples were run in duplicate and the average value was reported. The residues of the samples after the cone calorimetric test were photographed by a digital camera (PowerShot A2000 IS, Canon Inc., Japan).

2.4.11. Scanning electron microscopy-energy dispersive X-ray spectrometry (SEM-EDXS)

The morphology of the residual char was observed by a scanning electron microscope (EV0-18, Carl Zeiss Jena Co., Germany) with an accelerating voltage of 20.0 kV. The surface of the residual char was sputter-coated with a conductive gold layer before observation. EDXS result of the char was measured by an energy dispersive X-ray spectrometer.

2.4.12. Water solubility and water resistance test

Water solubility test: The sample (about 10 g) was put into 100 mL distilled water at a pre-set temperature and stirred at the temperature for 1 h. The suspension was then filtered. 50 mL of the filtrate was taken out and dried in a vacuum oven at 110 °C to a constant weight. The test was operated for five times and the average value was reported. The water solubility of the sample was calculated.

Water resistance test: The samples were immersed in distilled water at 70 °C and kept at this temperature for 168 h. The treated samples were subsequently taken out and dried in a vacuum oven at 70 °C to a constant weight. The weight of the sample was measured before water soaking and after drying. The migration percentage was calculated as the following equation (1):

$$\text{Migration Percentage} = \frac{(W_0 - W)}{W_0} \times 100\% \quad (1)$$

where W_0 is the initial weight of the samples before water soaking, and W is the remaining weight of the samples after water soaking and drying. Moreover, the water resistance of the composites was also evaluated by the change of LOI values and UL-94 vertical rating after the water treatment. All samples were operated for five times and the average value was reported.

Table 1
ICP-AES and elemental analysis data of PETBP.

	Element content (wt%)				
	P	C	N	O	H
Experimental value	10.26	39.55	21.69	24.83	3.67
Calculated value	9.91	38.34	22.36	25.56	3.83

Table 2
LOI and UL-94 vertical test results of the samples before and after soaking in 70 °C water for 168 h.

Samples	Before soaking		After soaking		Migration percentage (%)
	LOI (%)	UL-94 vertical rating	LOI (%)	UL-94 vertical rating	
PP	17.5	Failed	17.5	Failed	0
PP/PETBP (5wt%)	19.5	Failed	18.5	Failed	0.3
PP/PETBP (10wt%)	22.5	Failed	21.0	Failed	0.5
PP/PETBP (15wt%)	23.8	V-1	22.5	V-1	0.6
PP/PETBP (20wt%)	26.7	V-1	26.0	V-1	0.7
PP/PETBP (25wt%)	29.5	V-0	27.5	V-0	0.8
PP/PETBP (30wt%)	32.5	V-0	30.0	V-0	1.1
PP/TBM (25wt%)	24.0	Failed	23.0	Failed	1.7
PP/(MPP/TBM) (25wt%)	31.0	V-0	29.5	V-0	0.8
PP/(APP/PER) (25wt%)	29.0	V-0	26.0	Failed	4.5
PP/(APP/PER) (30wt%)	32.0	V-0	28.0	Failed	5.8

Note: the mass ratio of APP to PER was 3: 1, and the mass ratio of MPP to TBM was 2: 1.

3. Results and discussion

3.1. Characteration of PETBP

Fig. 1 shows the FTIR spectra of PEPA, cyanuric chloride (CNC) and PETBP. PEPA was mainly characterized by the following peaks: 3390 cm^{-1} (ν_{O-H}), 2960 and 2910 cm^{-1} (ν_{C-H}), 1299 cm^{-1} ($\nu_{P=O}$), 1019 cm^{-1}(ν_{P-O-C}) and 960 cm^{-1}(ν_{CH2-OH}) [19,20]. The characteristic peaks of CNC were listed as follows: 1502 cm^{-1} ($\nu_{-N=C-}$), 1269 cm^{-1} (ν_{C-N}), 849 cm^{-1} (ν_{tr-Cl}, tr meant triazine ring here) and 799 cm^{-1} (ν_{tr}) [15,17], while the spectrum of PETBP presented the following peaks: 3426 and 3250 cm^{-1} (ν_{N-H}), 2928 and 2863 cm^{-1} (ν_{C-H} of $-CH_2$-), 1501 cm^{-1} ($\nu_{-N=C-}$), 1336 cm^{-1} ($\nu_{tr.-N}$), 1299 cm^{-1} ($\nu_{P=O}$), 1269 cm^{-1} (ν_{C-N}), 1227 cm^{-1} (ν_{tr-O}), 1019 cm^{-1}(ν_{P-O-C}) and 799 cm^{-1} (ν_{tr}). The spectrum of PETBP contained most of the characteristic peaks of CNC, ethanediamine and PEPA. Besides, the peak at 849 cm^{-1} (ν_{C-Cl}) disappeared, whilst two new peaks located at 1336 cm^{-1} (ν_{tr-N}) and 1227 cm^{-1} (ν_{tr-O}) appeared, indicating the successful reaction of cyanuric chloride with PEPA and ethanediamine.

Fig. 2 displays the solid-state ^{13}C NMR spectrum of PETBP. The signal at chemical shifts of 166.7 ppm was assigned to the C atoms of the triazine ring [17,18]. The peak at 40.8 ppm was attributed to the $-CH_2-$ groups of the caged phosphate moiety. The signal located at 13.3 ppm was ascribed to the C atoms of the $-NH-\underline{C}H_2-$ groups. The peak at 8.9 ppm was corresponded to the quaternary

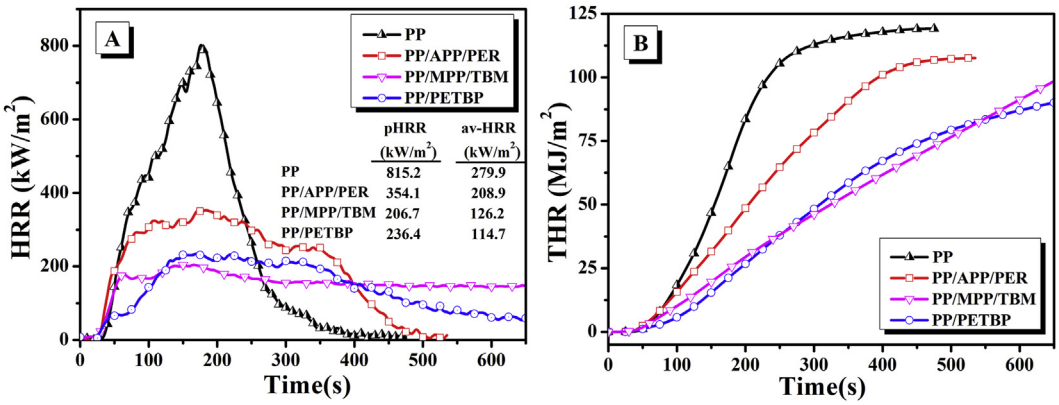

Fig. 4. Heat release rate (A) and total heat release (B) curves of PP and flame retardant PP. Note: the content of PETBP and APP/PER was 25wt%, respectively; the mass ratio of APP to PER was 3: 1, and the mass ratio of MPP to TBM was 2: 1.

carbon atoms in the caged phosphate moiety. The structure of PETBP was also confirmed by ^{31}P NMR spectrum illustrated in Fig. 3. One sharp signal was observed at −7.86 ppm, which was attributed to the phosphorus atom of the caged bicyclic phosphate.

To further confirm the structure of PETBP, inductively coupled plasma-atomic emission spectrometry (ICP-AES) was employed to detect the phosphorus (P) content, and the contents of carbon (C), nitrogen (N), oxygen (O) and hydrogen (H) were measured by elemental analyzer [21]. Table 1 lists the ICP-AES and EA data of PETBP. The content of P, C, N, O and H were 10.26 wt%, 39.55 wt%, 21.69 wt%, 24.83 wt% and 3.67 wt%, which were approximately in accordant with their calculated content, respectively. From the above analysis, it was confirmed that PETBP had been synthesized successfully.

3.2. Flame retardancy and water-resistance of flame retardant PP

Table 2 lists the LOI and UL-94 vertical test results of flame retardant PP before and after water soaking in 70 °C water for 168 h. The pure PP was highly flammable, and its LOI value was only 17.5%, and the UL-94 vertical test classed no rating. With increasing the PETBP content, the flame retardancy of the PP/PETBP mixture was gradually improved. When the content of PETBP was 25.0 wt%, the LOI value of the mixture was 29.5%, and the UL-94 vertical test classed a V-0 rating. Compared with the most commonly used intumescent flame retardant (IFR), i.e. ammonium polyphosphate/pentaerythritol (APP/PER), PETBP showed better flame-retardant efficiency and water resistance. When employing the same amount of the flame retardant, the PP/PETBP mixtures all showed better flame retardancy than the PP/APP/PER mixtures, no matter before or after water soaking. Table 2 also presents the migration percentages and the flame retardation changes of the samples after soaking in 70 °C water for 168 h. It is worth noting that after soaking in 70 °C water for 168 h, the PP/PETBP mixture showed low migration percentage and could still achieve UL-94 V-0 rating at 25.0 wt% PETBP content, whereas the PP/APP/PER mixture exhibited a much higher migration percentage and failed to pass the UL-94 vertical test even at 30.0 wt% IFR content. These might be explained by the fact that in comparison with the APP/PER system, PETBP was a single-component polymeric IFR; when being burned, its acid, blowing and charring moieties could interact with each other more closely and quickly, thus performing a better flame-retardant efficiency; moreover, PETBP had a higher molecular weight than PER or APP, hence it showed much lower solubility and better compatibility with PP [14,22].

Table 3
Characteristic parameters of the cone calorimetric test for PP and flame retardant PP.

Samples	PHRR (kW/m^2)	av-HRR (kW/m^2)	THR (MJ/m^2)	av-MLR (g/s·m^2)	pSPR (m^2/s)	TSP (m^2)	residue (%)
PP	815.2	279.9	119.0	0.087	0.091	14.3	0
PP/APP/PER	354.1	208.9	107.6	0.057	0.065	17.4	20.2
PP/MPP/TBM	206.7	126.2	97.8	0.031	0.052	13.8	15.7
PP/PETBP	236.4	114.7	82.3	0.029	0.045	12.2	21.8

Note: the content of PETBP, APP/PER and MPP/TBM was 25wt%, respectively; the mass ratio of APP to PER was 3: 1, and the mass ratio of MPP to TBM was 2: 1.

To further comparatively study the flame retardancy and water resistance of PETBP, the triazine-based macromolecule (TBM) containing intumescent flame retardant was also employed as a control sample. It could be seen that TBM used alone showed low flame retardancy. The LOI value of the PP/TBM mixture containing only 25.0 wt% TBM was 24.0%, and the UL-94 vertical test classed no rating. This was mainly because TBM was absent of acid source and difficult to form intumescent char, thus it could not effectively prevent the substrate from burning. When the content of melamine pyrophosphate (MPP) was 16.7 wt% and TBM was 8.3 wt%, the LOI value of the mixture reached 31.0% and classed a UL-94 V-0 rating. The PP/MPP/TBM mixture showed low migration percentage and could also achieve UL-94 V-0 rating after soaking in 70 °C water for 168 h. However, compared with PETBP, the combination of MPP and TBM in flame retardant PP required more complicated processing condition to achieve uniform dispersion of the IFR particles in the polymer.

In order to further investigate the flame retardancy of the mixtures in a real fire, cone calorimeter was employed to evaluate the combustion performance [23]. Fig. 4 illustrates the heat release rate (HRR) and total heat release (THR) curves of PP and flame retardant PP, and their characteristic parameters are listed in Table 3. It can be clearly seen that the pure PP burnt fiercely after ignition and a sharp peak appeared at 175s with the peak heat release rate (PHRR) as high as 815.2 kW/m^2, and it was burnt out within 455s. However, by adding 25 wt% PETBP, the PHRR, THR, average mass loss rate (av-MLR), smoke production rate (SPR) and total smoke production (TSP) of the mixture were considerably decreased. The PHRR, THR, av-MLR and TSP of the PP/PETBP mixture were 236.4 kW/m^2, 82.3 MJ/m^2, 0.029 g/s·m^2 and 12.2 m^2, which were 71.0%, 30.8%, 66.7% and 14.7% lower than those of the pure PP, respectively. This was mainly attributed to the fast formation of thick intumescent char, which was further confirmed by Fig. 12. When PP was ignited and burned, a compact intumescent char was formed timely by PETBP, which could effectively slow

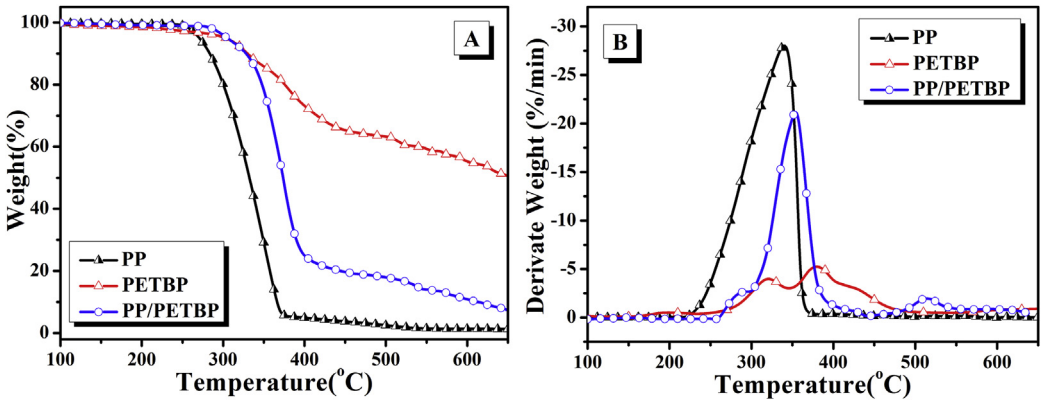

Fig. 5. TG (A) and DTG (B) curves of PP, PETBP and PP/PETBP. Note: the content of PETBP was 25wt%.

down the heat and combustible gaseous products transfer, thus protected the substrate from burning. In addition, compared with APP/PER and MPP/TBM, PETBP exhibited better flame retardancy. When using the same amount of the flame retardant additive, the PP/PETBP mixture showed lower av-HRR, THR, av-MLR and TSP than the PP/APP/PER and PP/MPP/TBM mixtures, indicating that PETBP showed higher efficiency in flame retardant PP, which was well in accordance with the results of LOI and UL-94 vertical test.

3.3. Thermal behavior and TG-FTIR analysis

TG and DTG curves of PP, PETBP and PP/PETBP are presented in Fig. 5. The results showed that the initial weight loss of the pure PP took place at 269 °C, with a maximum weight loss rate at 337 °C, and left no char residue at 700 °C. In the case of PETBP, it began to decompose at 290 °C, which was probably due to the scission of caged bicyclic phosphate and the formation of the compact swollen char [24]. The char residue of PETBP left at 700 °C was as high as 51.7wt%, indicating that PETBP possessed an outstanding char-forming capability. For the PP/PETBP mixture, the initial decomposition temperature (T_i, was defined as the temperature at which 5% mass loss occurred) and the maximum decomposition temperature (T_{max}) were 295 °C and 372 °C, which were 26 °C and 35 °C higher than those of PP, respectively. The residue char of the mixture left at 700 °C was 9.3 wt%. This could be explained by the fact that when being heated above 290 °C, PETBP was decomposed, cyclized and cross-linked to form a continuous intumescent char, which segregated the heat, oxygen and pyrolysis products transfer, thus prevented the substrate from decomposing and significantly improved the thermostability of the mixture [14].

In order to investigate the flame-retardant mechanism of PETBP, the gaseous pyrolysis products of PETBP were analyzed by TG-FTIR. Fig. 6 shows the 3D TG-FTIR spectra of pyrolysis products of PETBP during the thermal degradation, and the characteristic spectra obtained at different temperature are presented in Fig. 7. No obvious infrared signal could be observed below 250 °C, indicating that PETBP did not decompose below this temperature, thus it was thermally stable for melting-blend with PP. With further increasing the temperature, the release of H_2O (3400–4000 cm^{-1} and 1645 cm^{-1}), CO_2 (2340–2370 cm^{-1}), P–O–C (1075 cm^{-1}, phosphate ester fragment), NH_3 (930–960 cm^{-1}) and P–O–P (845 cm^{-1}, pyrophosphate fragment), etc. could be detected [25–27]. The phosphorus-containing compounds could quench the free radicals like H· and OH·, while the incombustible gases (H_2O, CO_2 and NH_3) diluted the flammable products and simultaneously reduced the heat of the flame [28]. When the temperature increased to 408 °C, a maximum signal intensity was observed. Subsequently, the signal intensity of the pyrolysis product decreased gradually, indicating that the decomposition rate of PETBP was slowed down by the char formation. Above 550 °C, only nonflammable gases composed of CO_2 and NH_3 could be observed, which might be attributed to the further decomposition of the unstable partial of the char residue [21].

To further understand the flame-retardant mechanism of PETBP in condense phase, the degradation residues at different temperature were investigated by FTIR. Fig. 8 displays the FTIR spectra of PETBP after heat treatment at different temperature for 15 min. At room temperature, the characteristic absorptions of PETBP were observed. There was no obvious difference of the characteristic bands for PETBP below 250 °C. By heating to 300 °C, the absorptions of N–H (3250–3700 cm^{-1}), C–H (2965, 2908 and 1473 cm^{-1}) and P–O–C (1019 cm^{-1}) became gradually weaker, which was ascribed to the degradation of phosphate esters (break of P–O–C bond) to form thermostable pyrophosphate [29]. Simultaneously, the –NH–CH_2– bond was destroyed and released NH_3. Above 400 °C, the bicyclic phosphate (870 cm^{-1}), $(RO)_3P{=}O$ (1299 cm^{-1}) and C–H bonds were destroyed, indicating the rapid decomposition of PETBP. Afterwards, the absorptions in the region 500–2000 cm^{-1} decreased quickly and almost vanished. However,

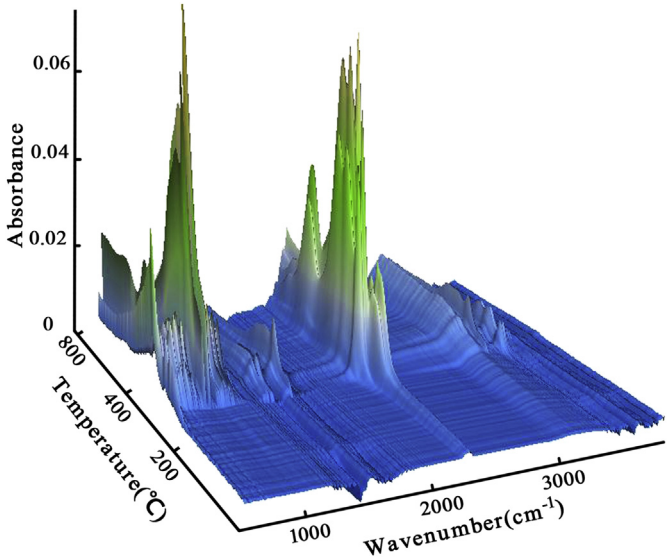

Fig. 6. 3D TG-FTIR spectra of pyrolysis products of PETBP during the thermal degradation.

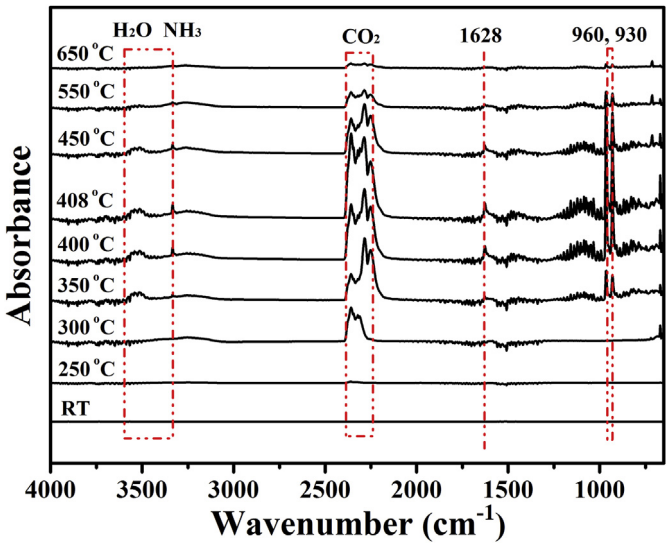

Fig. 7. FTIR spectra of pyrolysis products of PETBP at various temperatures.

it was worth noting that the absorptions at 1485 cm^{-1}($\nu_{-C=N-}$), 1299 cm^{-1} (ν_{P-O-C}), 1021 cm^{-1} ($\nu_{-C=O}$) and 800 cm^{-1} ($\nu_{tr.}$) remained apparent and could be still observed even at 650 °C, indicating that the dehydration and cross-linking reactions dominated the char-forming process, and the triazine rings were probably cross-linked by −P−O−C− bonds to form the thermostable graphite-like char [30].

In order to further clarify the flame-retardant mechanism of PETBP for PP, the gaseous pyrolysis products of PP and PP/PETBP at different temperatures were also analyzed by TG-FTIR. Fig. 9 shows the 3D TG-FTIR spectra of gaseous pyrolysis products of PP and PP/PETBP, and their characteristic spectra obtained at different temperature are shown in Fig. 10. For PP, it was hard to observe infrared signal below 300 °C. With the increase of temperature, the absorptions at about 3078 cm^{-1}, 2962 cm^{-1}, 1647 cm^{-1}, 1458 cm^{-1} and 1378 cm^{-1} were detected, which were attributed to the alkenes, dienes and alkanes released by PP [31]. Above 550 °C, almost all the absorptions disappeared, indicating that PP was decomposed completely. In comparison with PP, the degradation process of the PP/PETBP mixture was more complicated. PP/PETBP began to decompose at 300 °C, and its initial volatiles were mainly the nonflammable gases, such as H_2O (3400–4000 cm^{-1} and 1645 cm^{-1}), CO_2 (2340–2370 cm^{-1}) and NH_3 (930–960 cm^{-1}), etc. This was primarily because of the decomposition and dehydration of PETBP. Subsequently, the alkenes, dienes and alkanes decomposed by the polymer matrix were also observed. The maximum signal intensity of the PP/PETBP mixture appeared at about 499 °C, which was 28 °C higher than that of PP, indicating that PETBP could effectively enhance the thermostability of PP, which was in accordance with the TG analysis. This could be explained by the formation of an intumescent char which prevented the matrix from decomposition. Above 550 °C, the signal intensity of the gaseous pyrolysis products decreased gradually, indicating that the decomposition rate of the mixture was slowed down by the promoted char formation.

Hydrocarbons are the main decomposed products of PP, and also important parts of combustible gases. Fig. 11 presents the evolution curves of hydrocarbons, which are shown as the infrared absorbance at 2964 cm^{-1} versus temperature, respectively. It was worth noting that the initial hydrocarbons gases release for PP/PETBP occurred at 372 °C, which was 51 °C higher than that of PP. This might be because that the decomposition of PETBP generated phosphorus-containing compounds radicals including phosphate ester radicals and pyrophosphate radicals (mainly the P−O· radicals), which could quench the free radicals and promoted the thermostability of the polymer. Furthermore, the maximum intensity temperature of hydrocarbons from PP/PETBP was 28 °C higher than that of PP, while the intensity of the hydrocarbons decomposed by the former was much lower than that of the later. The reason was that the incombustible gases (H_2O, CO_2 and NH_3) decomposed by PETBP took away part of the heat; meanwhile, a swollen char was formed and prevented the mixture from decomposition.

3.4. Morphology and SEM-EDXS analysis of the residue char

The quality of the intumescent char is considered to be one of the most important factors determining the flame-retardant efficiency [32,33]. Understanding the morphology and composition of the char layer is beneficial to further clarify the flame-retardant mechanism. Fig. 12 shows the digital photographs and SEM-EDXS image of the residue char for the PP/PETBP mixture after cone calorimetric test. It could be clearly seen that a continuous, thick and compact swollen char was formed and covered on the substrate (Fig. 12a–c). The expansion ratio of the char layer was quite high, indicating that the decomposed gases could hardly permeate through the char layer [21]. The intumescent char layer acted as a good barrier to segregate the heat, oxygen and combustible gas transfer. Therefore, it could effectively reduce the heat release rate, mass loss rate and smoke production rate of the mixture. The micromorphology and composition of the char layer were also observed by the scanning electron microscopy-energy dispersive X-ray spectrometry (SEM-EDXS). As shown in Fig. 12d, a continuous, dense and compact outer surface could be seen, and its chemical compositions included 36.5 wt% carbon (C), 41.8 wt% oxygen (O), 10.2 wt% nitrogen (N) and 11.5wt% phosphorus (P). The high C, N and P contents of the residue suggested that C atoms probably were cross-linked with P and N atoms to form a thermostable char [34].

3.5. Possible flame-retardant mechanism

Based on the results analyzed above, a possible flame-retardant mechanism of PETBP is illustrated in Fig. 13. When the temperature

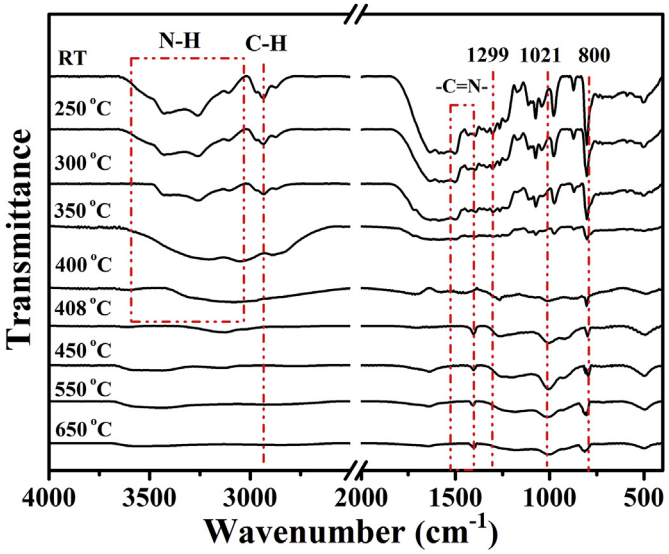

Fig. 8. FTIR spectra of PETBP after heat treatment at different temperature for 15 min.

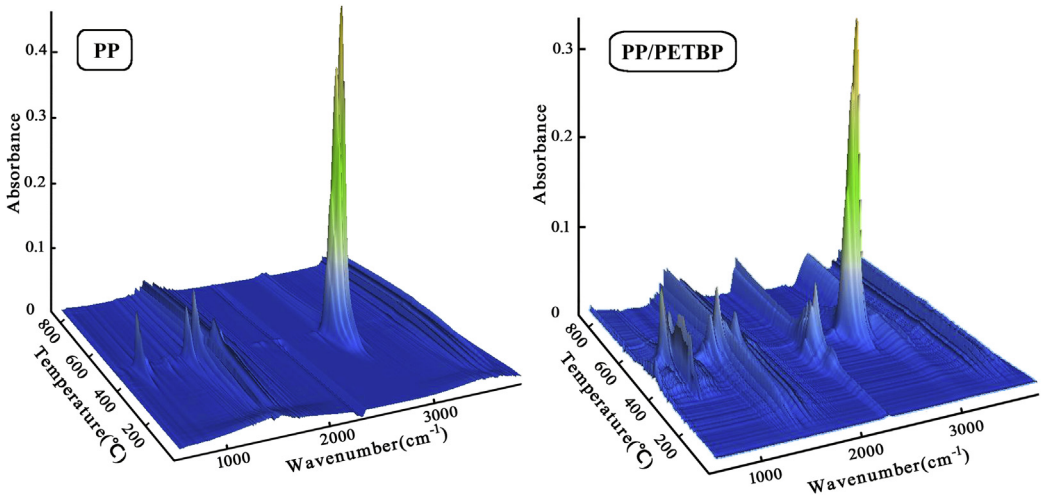

Fig. 9. 3D TG-FTIR spectra of gaseous pyrolysis products of PP and PP/PETBP during the thermal degradation. Note: the content of PETBP was 25wt%.

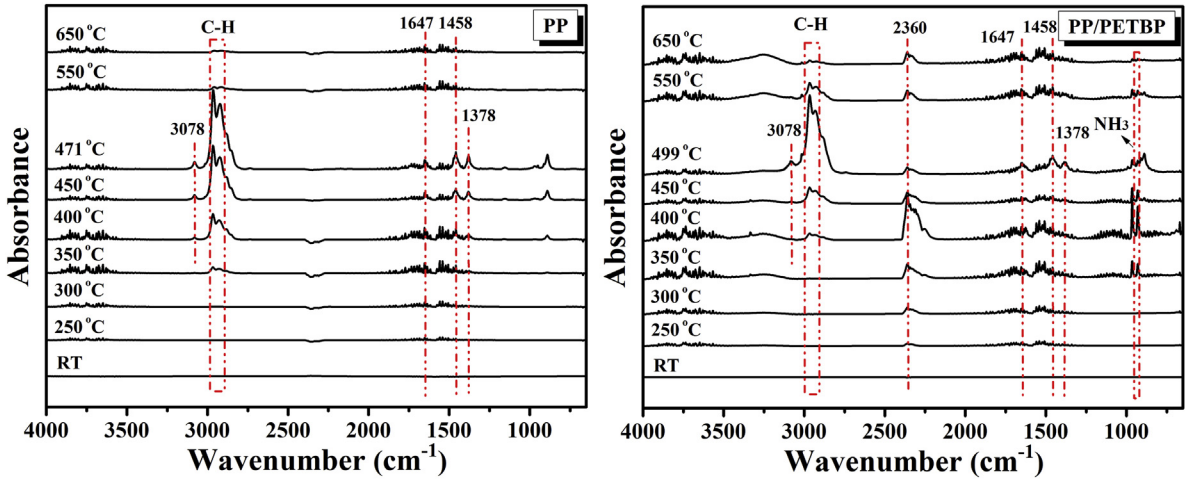

Fig. 10. FTIR spectra of gaseous pyrolysis products of PP and PP/PETBP at different temperatures. Note: the content of PETBP was 25wt%.

reached above 290 °C, PETBP began to decompose and released NH_3 and H_2O. The main decomposition products were triazine oligomer radicals and phosphorus-containing compound radicals (mainly the P—O· radicals) including phosphate ester radicals and pyrophosphate radicals, which could inhibit the free radicals produced by the polymer; meanwhile, the incombustible gases (H_2O and NH_3) diluted the combustible gas and reduced the heat of the flame. With the increase of temperature, the triazine oligomers and phosphorus-containing compounds formed the precursor of intumescent char *via* cyclization. Afterwards, the char precursor was further cross-linked and foamed by H_2O, CO_2 and NH_3. As a result, an intumescent char was formed and covered on the matrix. The char layer was continuous, compact and thermally stable, which could effectively segregate the heat, oxygen and combustible gas transfer, thus protected the substrate material from burning.

4. Conclusion

An efficient single-component polymeric intumescent flame retardant PETBP was synthesized and characterized. PETBP could significantly improve the flame retardancy and thermostability of PP. When the content of PETBP was 25.0 wt%, the PP/PETBP mixture could achieve a limiting oxygen index (LOI) value of 29.5% and a UL-

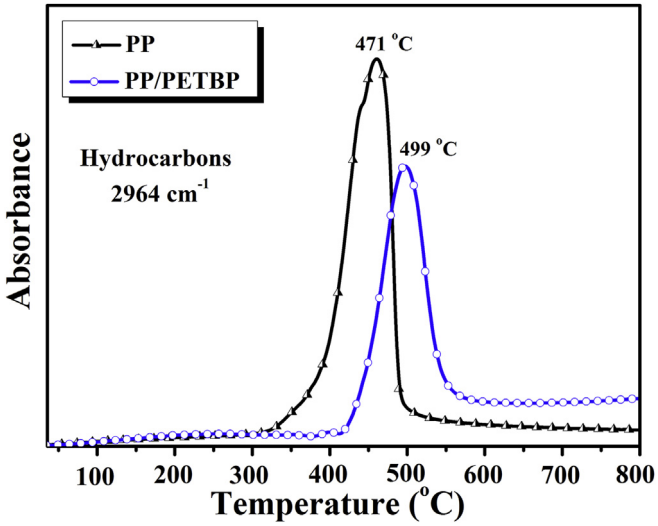

Fig. 11. FTIR absorbance vs. temperature curves of hydrocarbons evolved from PP and PP/PETBP. Note: the content of PETBP was 25wt%.

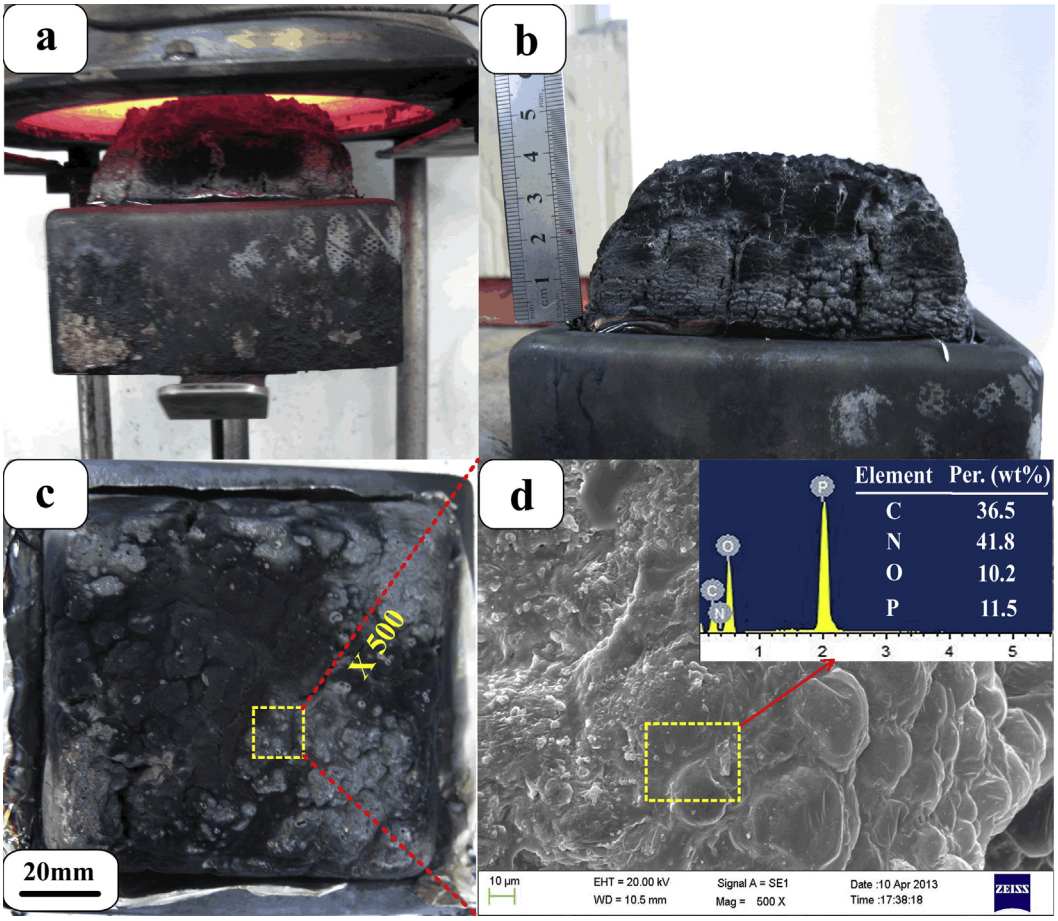

Fig. 12. Digital photographs (a–c) and SEM-EDXS image (d) of the char residue for the PP/PETBP composite after the cone calorimetric test. Note: the content of PETBP was 25wt%.

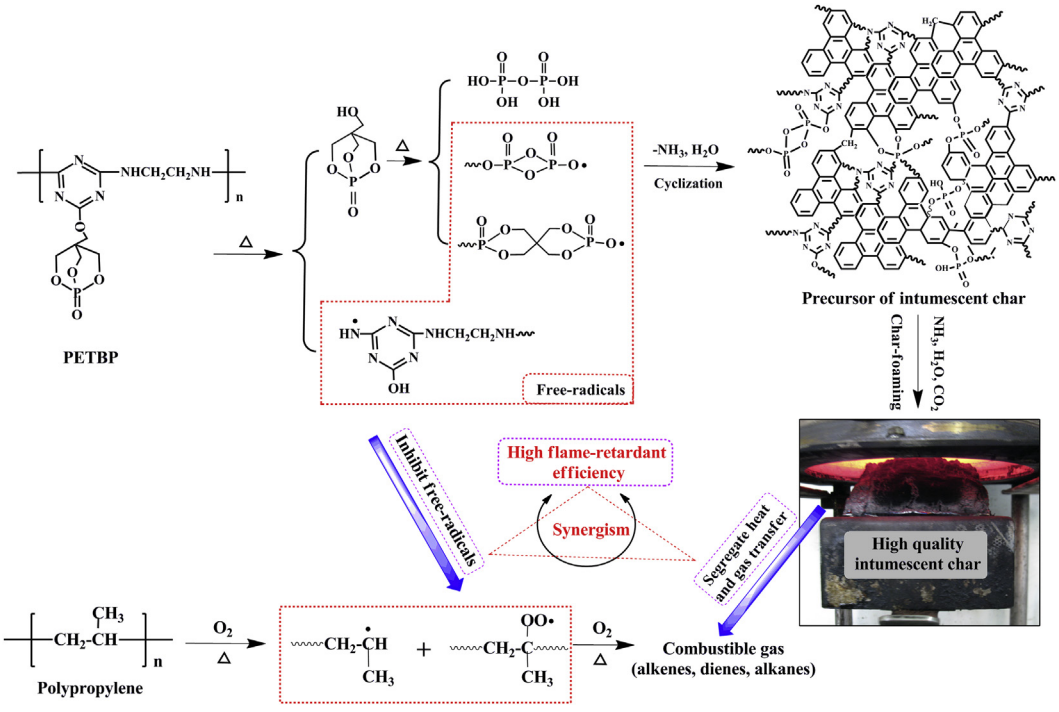

Fig. 13. Possible flame-retardant mechanism of PETBP for PP.

94 V-0 rating, and it could still maintain a UL-94 V-0 rating after soaking in 70 °C water for 168 h. In addition, the peak heat release rate (PHRR), total heat release (THR) and average mass lose rate (av-MLR) were also considerably decreased. TGA, TG-FTIR and SEM-EDXS results revealed that during the combustion, PETBP could generate the phosphorus-containing compound radicals and inhibit the free radicals of PP chain scission; afterwards, a high quality and thermally stable intumescent char was formed and covered on the matrix, slowing down the heat, oxygen and combustible gas transfer, thus effectively protected the polymer from burning.

Acknowledgments

We gratefully acknowledge the financial supports by the Guangdong Natural Science Foundation (S2013040015249), the China Postdoctoral Science Foundation (2014M560660) and the Fundamental Research Funds for the Central Universities (2013ZB0007).

References

[1] Bourbigot S, Lebras M, Duquesne S, Rochery M. Recent advances for intumescent polymers. Macromol Mater Eng 2004;289(6):499–511.
[2] Wang JJ, Wang L, Xiao AG. Recent research progress on the flame-retardant mechanism of halogen-free flame retardant polypropylene. Polym Plast Technol 2009;48(3):297–302.
[3] Liu Y, Wang Q. Synthesis of in situ encapsulated intumescent flame retardant and the flame retardancy in polypropylene. Polym Compos 2007;28(2):163–7.
[4] Camino G, Costa L, Martinasso G. Intumescent fire-retardant systems. Polym Degrad Stab 1989;23(4):359–76.
[5] Camino G, Costa L, Luda di Cortemiglia MP. Overview of fire retardant mechanisms. Polym Degrad Stab 1991;33(2):131–54.
[6] Bourbigot S, Lebras M, Delobel R. Carbonization mechanisms resulting from intumescence association with the ammonium polyphosphate-pentaerythritol fire retardant system. Carbon 1993;31(8):1219–30.
[7] Chen YH, Liu Y, Wang Q, Yin H, Aelmans N, Kierkels R. Performance of intumescent flame retardant master batch synthesized through twin-screw reactively extruding technology: effect of component ratio. Polym Degrad Stab 2003;81(2):215–24.
[8] Wang Q, Chen YH, Liu Y, Yin H, Aelmans N, Kierkeis R. Performance of an intumescent-flame-retardant master batch synthesized by twin-screw reactive extrusion: effect of the polypropylene carrier resin. Polym Int 2004;53(4):439–48.
[9] Liu MF, Liu Y, Wang Q. Flame-retarded poly(propylene) with melamine phosphate and pentaerythritol/polyurethane composite charring agent. Macromol Mater Eng 2007;292(2):206–13.
[10] Wu K, Wang ZZ, Liang HJ. Microencapsulation of ammonium polyphosphate: preparation, characterization, and its flame retardance in polypropylene. Polym Compos 2008;29(8):854–60.
[11] Ni JX, Tai QL, Lu HD, Hu Y, Song L. Microencapsulated ammonium polyphosphate with polyurethane shell: preparation, characterization, and its flame retardance in polyurethane. Polym Adv Technol 2010;21(6):392–400.
[12] Tai QL, Shan XY, Song L, Lo SM, Yuen RKK, Hu Y. A polymeric flame retardant and surfactant-free montmorillonite nanocomposites: preparation and exfoliation mechanism discussion. Polym Compos 2014;35(1):167–73.
[13] Tian NN, Gong J, Wen X, Yao K, Tang T. Synthesis and characterization of a novel organophosphorus oligomer and its application in improving flame retardancy of epoxy resin. RSC Adv 2014;4(34):17607–14.
[14] Song PA, Fang ZP, Tong LF, Xu ZB. Synthesis of a novel oligomeric intumescent flame retardant and its application in polypropylene. Polym Eng Sci 2009;49(7):1326–31.
[15] Hu XP, Li WY, Wang YZ. Synthesis and characterization of a novel nitrogen-containing flame retardant. J Appl Polym Sci 2004;94(4):1556–61.
[16] Li B, Xu MJ. Effect of a novel charring-foaming agent on flame retardancy and thermal degradation of intumescent flame retardant polypropylene. Polym Degrad Stab 2006;91(6):1380–6.
[17] Dai JF, Li B. Synthesis, thermal degradation, and flame retardance of novel triazine ring-containing macromolecules for intumescent flame retardant polypropylene. J Appl Polym Sci 2010;116(4):2157–65.
[18] Lai XJ, Zeng XR, Li HQ, Liao F, Yin CY, Zhang HL. Synergistic effect between a triazine-based macromolecule and melamine pyrophosphate in flame retardant polypropylene. Polym Compos 2012;33(1):35–43.
[19] Halpern Y, Mott DM, Niswander RH. Fire retardancy of thermoplastic materials by intumescence. Ind Eng Chem Prod Res Dev 1984;23(2):233–8.
[20] Sarannya V, Sivasamy P, Mathan ND, Rajkumar T, Ponraju D, Vijayakumar CT. Study of thermal properties of intumescent additive. J Therm Anal Calorim 2010;102(3):1071–7.
[21] Xu ZZ, Huang JQ, Chen MJ, Tan Y, Wang YZ. Flame retardant mechanism of an efficient flame-retardant polymeric synergist with ammonium polyphosphate for polypropylene. Polym Degrad Stab 2013;98(10):2011–20.
[22] Dasari A, Yu ZZ, Cai GP, Mai YW. Recent developments in the fire retardancy of polymeric materials. Prog Polym Sci 2013;38(9):1357–87.
[23] Tang G, Huang XJ, Ding HC, Wang X, Jiang SD, Zhou KQ, et al. Combustion properties and thermal degradation behaviors of biobased polylactide composites filled with calcium hypophosphite. RSC Adv 2014;4(18):8985–93.
[24] Horrocks AR, Price D, editors. Fire retardant materials. Boca Raton: Woodhead Publishing CRC Press; 2001.
[25] Wu K, Hu Y, Song L, Lu HD, Wang ZZ. Flame retardancy and thermal degradation of intumescent flame retardant starch-based biodegradable composites. Ind Eng Chem Res 2009;48(6):3150–7.
[26] Wu K, Kandola BK, Kandare E, Hu Y. Flame retardant effect of polyhedral oligomeric silsesquioxane and triglycidyl isocyanurate on glass fibre-reinforced epoxy composites. Polym Compos 2011;32(3):378–89.
[27] Wu N, Yang RJ. Effects of metal oxides on intumescent flame-retardant polypropylene. Polym Adv Technol 2011;22(5):495–501.
[28] Chen WL, Fu XW, Ge WB, Xu JJ, Jiang MJ. Microencapsulation of bisneopentyl glycol dithiopyrophosphate and its flame retardant effect on polyvinyl alcohol. Polym Degrad Stab 2014;102:81–7.
[29] Jiang WZ, Hao JW, Han ZD. Study on the thermal degradation of mixtures of ammonium polyphosphate and a novel caged bicyclic phosphate and their flame retardant effect in polypropylene. Polym Degrad Stab 2012;97(4):632–7.
[30] Qian XD, Song L, Hu Y, Yuen RKK, Chen LJ, Guo YQ, et al. Combustion and thermal degradation mechanism of a novel intumescent flame retardant for epoxy acrylate containing phosphorus and nitrogen. Ind Eng Chem Res 2011;50(4):1881–92.
[31] Zhang F, Zhang J, Sun DX. Study on Thermal decomposition of intumescent fire-retardant polypropylene by TG/Fourier transform infrared. J Thermoplast Compos 2009;22(6):681–701.
[32] Nie SB, Song L, Bao CL, Qian XD, Guo YQ, Hong NN, et al. Synergistic effects of ferric pyrophosphate (FePP) in intumescent flame-retardant polypropylene. Polym Adv Technol 2011;22(6):870–6.
[33] Lai XJ, Zeng XR, Li HQ, Zhang HL. Effect of polyborosiloxane on the flame retardancy and thermal degradation of intumescent flame retardant polypropylene. J Macromol Sci B 2014;53(4):721–34.
[34] Chen J, Liu SM, Zhao JQ. Synthesis, application and flame retardancy mechanism of a novel flame retardant containing silicon and caged bicyclic phosphate for polyamide 6. Polym Degrad Stab 2011;96:1508–15.